

Table 1 Absorbency of Dye 1 at λ_{\max}

Concentration $\times 10^6$ /mol/L	Temperature / $^{\circ}\text{C}$			
	25.0	30.5	35.5	41.0
2.04	0.2971	0.2941	0.2877	0.2813
4.08	0.5707	0.5645	0.5592	0.5530
5.75	0.7906	0.7814	0.7745	0.7673
7.68	1.0302	1.0404	1.0297	1.0222
9.67	1.2705	1.2982	1.2836	1.2729

(SHIMADZU CORPORATION), in which the specimen chamber temperature was controlled by a Superther-mostat-501 (SHANGHAI ANALYTICAL INSTRUMENT FACTORY).

The three benzindocarbocyanine dyes were synthesized according to the literatures.¹ The methanol used was of analytical reagent grade. Three stock solutions (1×10^{-4} mol/L) were prepared by dissolving these solid dyes in methanol. Immediately before use, the solutions were diluted with water and/or methanol to a 50 volume % aqueous methanol solutions.

Results and Discussion

Thermodynamics of three kinds of benzindocarbocyanine dyes. The formation of molecular aggregation state is influenced and controlled by many factors, among which the structure of dye molecule, temperature and concentration are important. There are several different types of aggregates in solution of cyanine dye, and there is a dynamic reversible equilibrium between aggregate and monomer.

Table 1 lists the absorbency of Dye 1 at λ_{\max} of different temperatures and concentrations. It can be found that the absorption of Dye 1 at the same concentration is decreased with an increase of temperature, but the range of change is not great. The results show that Dye 1 has better thermal stability.

Fig. 1 shows the absorption spectra of Dye 1 solutions of five different concentrations in 50 volume % aqueous methanol solutions at 25 $^{\circ}\text{C}$. From Fig. 1, we can see that there are two absorption peaks in visible range for Dye 1 in 50 volume % aqueous methanol solutions. The peaks at 587 and 550 nm can be assigned to monomer (M) band and aggregation (H) band, respectively. The absorption intensity of aggregation (H) relative to the monomer band enhances with increasing dye concentration. It can be also found that the absorption wavelength of Dye 1 with the same concentration at different temperatures is the same (Fig. 2). The results show that Dye 1

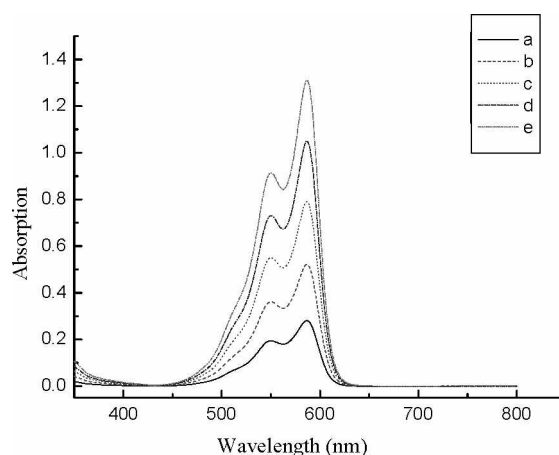


Figure 1. Absorption spectra of Dye 1 in 50 volume % aqueous methanol solutions at 25 $^{\circ}\text{C}$: a: 2.04×10^{-6} mol/L, b: 4.08×10^{-6} mol/L, c: 5.75×10^{-6} mol/L, d: 7.68×10^{-6} mol/L, e: 9.67×10^{-6} mol/L

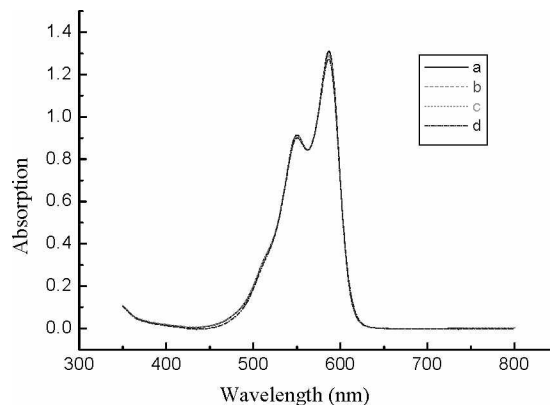


Figure 2. Absorption spectra of Dye 1 (concentration: 9.67×10^{-6} mol/L) in 50 volume % aqueous methanol solutions: a: 25.0 $^{\circ}\text{C}$, b: 30.5 $^{\circ}\text{C}$, c: 35.5 $^{\circ}\text{C}$, d: 41.0 $^{\circ}\text{C}$

may exist an equilibrium between monomer and dimer in 50 volume % aqueous methanol solutions between 25.0 $^{\circ}\text{C}$ to 41.0 $^{\circ}\text{C}$.¹⁷ That is, the main peak at 587 nm is ascribed to monomer (M) band and the shoulder peak at 550 nm is dimer band (D). The aggregation behavior of Dye 2 and Dye 3 is similar with Dye 1, existing the equilibrium between monomer and dimer in 50 volume % aqueous methanol solutions between 28.0 $^{\circ}\text{C}$ to 44.0 $^{\circ}\text{C}$ and between 26.0 $^{\circ}\text{C}$ to 47.0 $^{\circ}\text{C}$, respectively.

To determine the dimeric aggregation constant K_D and the molar absorption coefficient ϵ_M of the monomer simul-

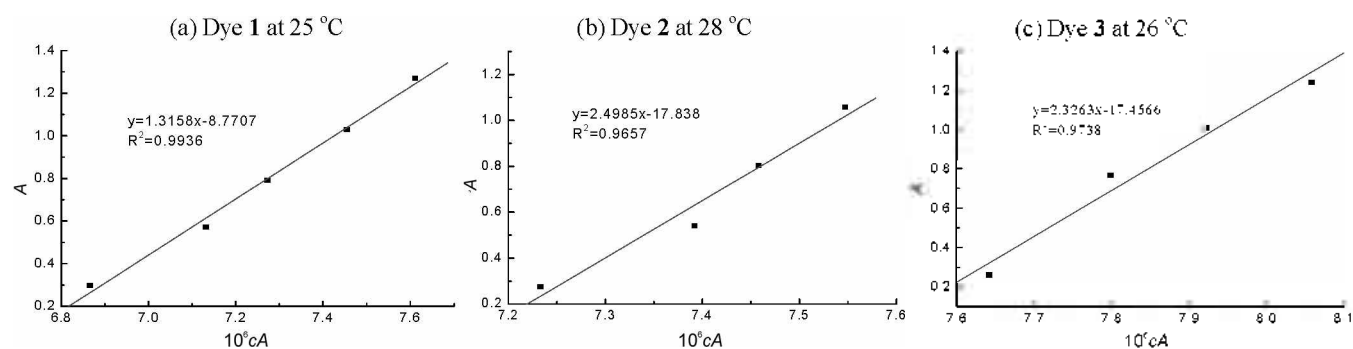
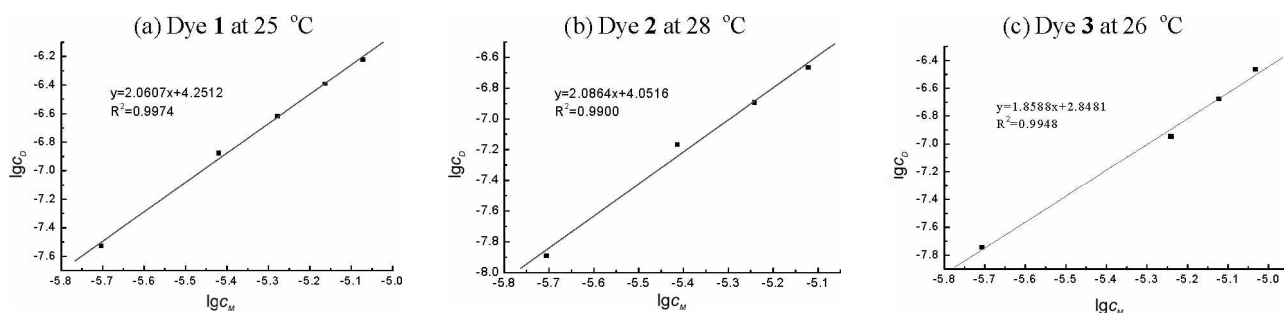
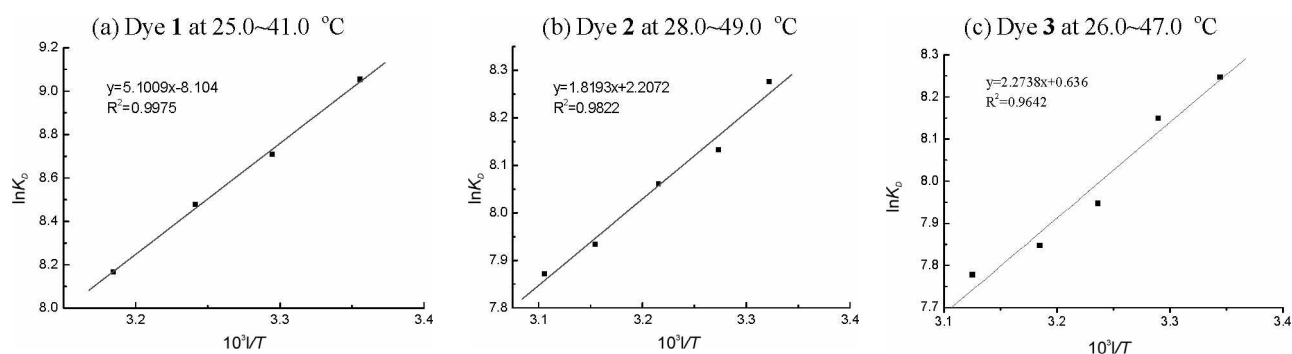


Figure 3. Correlation of A with c/A for three dyes

Figure 4. Correlation of $\lg c_D$ with $\lg c_M$ for three dyesFigure 5. Correlation of $\ln K_D$ with $1/T$ for three dyes

taneously from the dependence of monomer band absorbance A on total dye concentration c , according to the Harris and Hobbs,^{14,18} we have

$$A = (\epsilon_M^2 l^2 / 2K_D) (c/A) - \epsilon_M l / 2K_D \quad (1)$$

where l represents solution thickness and c , the total dye

Table 2. Thermodynamic parameters of dimerization of Dye 1 in 50 volume % aqueous methanol solutions

Temperature / °C	$K_D \times 10^{-3}$ / L·mol ⁻¹	$\epsilon_M \times 10^{-5}$ / L·mol ⁻¹ ·cm ⁻¹	Association number n	ΔG_D / kJ·mol ⁻¹	ΔH_D / kJ·mol ⁻¹	ΔS_D / J·mol ⁻¹ ·K ⁻¹
25.0	8.55	1.50	2.1	-22.4	-42.5	-67.3
30.5	6.05	1.47	1.9	-22.0	-42.5	-67.6
35.5	4.80	1.43	2.1	-21.7	-42.5	-67.2
41.0	3.52	1.40	2.0	-21.3	-42.5	-67.4

Table 3. Thermodynamic parameters of dimerization of Dye 2 in 50 volume % aqueous methanol solutions

Temperature / °C	$K_D \times 10^{-3}$ / L·mol ⁻¹	$\epsilon_M \times 10^{-5}$ / L·mol ⁻¹ ·cm ⁻¹	Association number n	ΔG_D / kJ·mol ⁻¹	ΔH_D / kJ·mol ⁻¹	ΔS_D / J·mol ⁻¹ ·K ⁻¹
28.0	3.93	1.40	2.1	-20.7	-15.1	18.5
32.5	3.40	1.38	2.1	-20.7	-15.1	18.1
38.0	3.17	1.36	2.1	-20.8	-15.1	18.4
44.0	2.79	1.35	2.1	-20.9	-15.1	18.2
49.0	2.62	1.34	2.0	-21.1	-15.1	18.5

Table 4. Thermodynamic parameters of dimerization of Dye 3 in 50 volume % aqueous methanol solutions

Temperature / °C	$K_D \times 10^{-3}$ / L·mol ⁻¹	$\epsilon_M \times 10^{-5}$ / L·mol ⁻¹ ·cm ⁻¹	Association number n	ΔG_D / kJ·mol ⁻¹	ΔH_D / kJ·mol ⁻¹	ΔS_D / J·mol ⁻¹ ·K ⁻¹
26.0	3.82	1.33	1.9	-20.5	-18.9	5.4
31.0	3.46	1.32	1.9	-20.6	-18.9	5.6
36.0	2.83	1.31	2.0	-20.4	-18.9	4.9
41.0	2.56	1.29	1.9	-20.5	-18.9	5.1
47.0	2.39	1.27	1.9	-20.7	-18.9	5.6

concentration. As is shown in Fig. 3, the dependence of A on c/A shows a straight line relationship. Both the slope $\varepsilon_M^2 F^2 / 2K_D$ and intercept $-\varepsilon_M / 2K_D$ are used to determine K_D and ε_M , which are $8.55 \times 10^3 \text{ L}\cdot\text{mol}^{-1}$ and $1.50 \times 10^5 \text{ L}\cdot\text{mol}^{-1}\cdot\text{cm}^{-1}$ for Dye 1 at 25 °C, $3.93 \times 10^3 \text{ L}\cdot\text{mol}^{-1}$ and $1.40 \times 10^5 \text{ L}\cdot\text{mol}^{-1}\cdot\text{cm}^{-1}$ for Dye 2 at 28 °C, $3.82 \times 10^3 \text{ L}\cdot\text{mol}^{-1}$ and $1.33 \times 10^5 \text{ L}\cdot\text{mol}^{-1}\cdot\text{cm}^{-1}$ for Dye 3 at 26 °C in 50 volume % aqueous methanol solution, respectively.

Concentrations of monomers c_M and of dimers $c_D = (c - c_M) / 2$ are calculated using either ε_M and A or K_D and c . A conventional plot of $\log c_D$ versus $\log c_M$ gives a straight line of slope approximately 2.0, as shown in Fig. 4, confirming that there is all an equilibrium between monomers and dimers in the three dyes solution, which can be described as



Therefore

Table 5. Selected bond lengths(Å), bond angles (°) and dihedral angles (°) of dyes

	Dye 1	Dye 2	Dye 3
Bond lengths			
1, 2	1.477	1.477	1.435
2, 4	1.365	1.365	1.364
3, 4	1.550	1.545	1.544
4, 5	1.399	1.399	1.398
5, 6	1.399	1.400	1.401
6, 7	1.401	1.400	1.398
7, 8	1.400	1.400	1.400
8, 9	1.365	1.364	1.364
9, 10	1.477	1.477	1.477
8, 11	1.545	1.545	1.547
Bond angles			
2, 4, 3	108.3	108.5	108.4
2, 4, 5	123.1	122.5	121.9
4, 5, 6	127.4	127.2	127.1
5, 6, 7	122.6	122.7	122.7
7, 8, 9	122.5	122.5	123.1
Dihedral angles			
1, 2, 4, 3	178.8	179.6	179.7
1, 2, 4, 5	1.1	0.2	0.4
3, 4, 5, 6	1.0	0.8	0.6
2, 4, 5, 6	178.8	179.3	179.6
6, 7, 8, 9	179.5	179.0	178.7
6, 7, 8, 11	0.1	0.8	1.2
7, 8, 9, 10	0.1	0.4	179.9

$$K_D = c_D / c_M^2 \quad (3)$$

The K_D values at different temperatures allow us to calculate ΔH_D , according to the Van't Hoff equation:

$$d \ln K_D / d(1/T) = -\Delta H_D / R \quad (4)$$

where $R = 8.31 \text{ J mol}^{-1} \text{ K}^{-1}$ the universal gas constant, and T the Kelvin temperature. The plot of $\ln K_D$ versus $1/T$, as shown in Fig. 5, shows a straight line. From its slope the ΔH_D is calculated to be -42.5 kJ/mol for Dye 1 at 25.0 ~ 41.0 °C, -15.1 kJ/mol for Dye 2 at 28.0 ~ 49.0 °C and -18.9 kJ/mol for Dye 3 at 26.0 ~ 47.0 °C in 50 volume % aqueous methanol solutions.

The ΔG_D and ΔS_D values were obtained according to thermodynamic equations $\Delta G_D = -RT \ln K_D$ and $\Delta S_D = (\Delta H_D - \Delta G_D) / T$. These data were listed in Table 2 for Dye 1, Table 3 for Dye 2 and Table 4 for Dye 3.

Computational

Geometric structures. In this work, the ground-state geometries were fully optimized using DFT at B3LYP/6-31G level. Analytic frequency calculations were done and the frequency possessed no imaginary frequency. It confirmed the optimized structures to be an energy minimum. All calculations reported in this work were carried out with the GAUSSIAN 03 program. The geometries and atomic numbering of three kinds of benzindocarbocyanine dyes show in Scheme 1.

Table 5 lists some selected bond lengths, bond angles and selected dihedral angles for the three kinds of dye molecules. It can be found that the carbon-carbon bond lengths on the dye molecular skeleton are basically intermediate between typical C-C single (1.54 Å) and C=C double (1.34 Å) bonds, and carbon-nitrogen bond lengths are also intermediate between C-N typical single (1.47 Å) and C=N double (1.27 Å) bonds. All C-C-C, C-N-C and C-C-N bond angles are close to 120°. It indicates that the π electrons in the dye molecule are delocalized. The dihedral angles on the dye molecular skeleton are close to 180° or 0°. It indicates that the main atoms are kept in the same plane. The structure of geometrical monomer optimization according to the B3LYP/6-31G level show in Fig. 6.

The effect of dye molecule structure on aggregation behavior: From Table 2, Table 3 and Table 4, it can be found that the dimeric enthalpy ΔH_D values of three dyes are all negative, and the sequence of ΔH_D in the nearly same temperature and concentration range is Dye 1 < Dye 3, Dye 2. That is, the

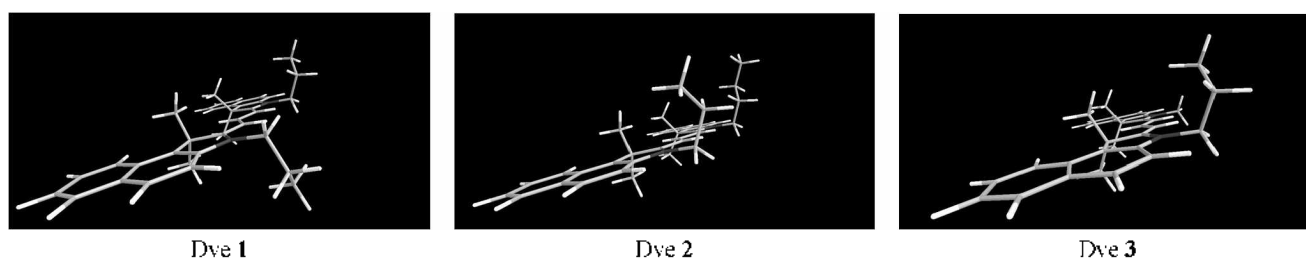


Figure 6. The structure of geometrical monomer optimization according to the B3LYP/6-31G level

dimeric association of Dye **1** is easier than Dye **3** and Dye **2**. The reason suggested here is that Dye **1** has a planar structure, and the two propyls attached to N or N⁺ are on the opposite sides of the plane (Fig. 6), which is fit for molecular ordered arrangement and forming a face-to-face and head-to-tail π -electrons stack with zipper structure.¹⁹ Dye **3** has also a planar structure, and the methyl attached to N or N⁺ is in this plane but the propyl attached to N or N⁺ is not, although it can form a face-to-face and head-to-tail π -electrons stack, the stack is not zipper structure. Dye **2** has also a planar structure, but the propyl and butyl attached to N or N⁺ are on the same side of the plane, so the activity of forming a face-to-face and head-to-tail π -electrons stack is decreased due to steric hindrance.

Conclusion

The spectrophotometric determination of thermodynamic parameters of three kinds of benzindocarbocyanine dyes: Dye **1**, Dye **2** and Dye **3** in 50 volume % aqueous methanol solution is reported. The dimeric association constant K_D , the dimeric free energy ΔG_D , the dimeric entropy ΔS_D , and the dimeric enthalpy ΔH_D were obtained. The effect of dye molecule structure on ΔH_D is also discussed by theoretical calculations.

Acknowledgments. We appreciate the financial support for this research by a grant from the Natural Science Foundation of Shaanxi Province (No. SJ08B04), the Special Science Research Foundation of Education Committee (No. 08JK458) and the Science Research Startup Foundation of Northwest University.

References

- Mishra, A.; Behera, R. K.; Behera, P. K.; Mishra, B. K.; Behera, G. B. *Chemical Review* **2000**, *100*, 1973.
- Lin, Y. H.; Weissleder, R.; Tung, C. H. *Bioconjugate Chem.* **2002**, *13*, 605.
- Mader, O.; Reiner, K.; Egelhaaf, H. J.; Fischer, R.; Brock, R. *Bioconjugate Chem.* **2004**, *15*, 70.
- He, G. S.; Bhawalker, J. D.; Shao, C. F. *Appl. Phys. Lett.* **1995**, *65*, 2433.
- He, G. S.; Signomii, R.; Prasad, P. N. *IEEE J Quantum Electron* **1998**, *34*, 7.
- Gan, F.-X. *Digital Optical Disks and Optical Storage Media*; Shanghai Science and Technology Press: Shanghai, 1992.
- Zhang, Z.-X.; Zhang, Y.-J.; Hao, J.-X.; Zhang, Z.-J. *Sci. China (Ser B)* **1995**, *25*, 689.
- Zhang, C.-L.; Wang, L.-Y.; Zhang, X.-H.; Zhang, Z.-X.; Cao, Z.-X. *J. Funct Mater.* **2001**, *32*, 546.
- Wang, L.-Y.; Zhang, X.-G.; Shi, Y.-P.; Zhang, Z.-X. *Dyes Pigments* **2004**, *21*.
- Fan, F.-L.; Wang, L.-Y.; Yuan, H.-A.; Zhang, Z.-X. *Chemical Engineering* **2007**, *35*, 63.
- Li, C.-L.; Wang, L.-Y.; Sun, G.-F.; Zhang, Z.-X. *Chinese Journal of Organic Chemistry* **2006**, *26*, 442.
- Fan, F.-L.; Wang, L.-Y.; Yuan, H.-A.; Zhang, Z.-X. *Chemistry* **2005**, *68*, w102.
- Niazi, A.; Yazdanipour, A.; Ghasemi, J.; Kubista, M. *Spectrochim. Acta Part A* **2006**, *65*, 73.
- Zhang, Z.-J.; Hao, J.-X.; Wu, B.-Y.; Yuan, H.-A. *Journal of Imaging Science and Technology* **1995**, *39*, 373.
- Matsubara, T.; Tanaka, T. *J. Imaging Sci.* **1991**, *35*, 274.
- Meng, F.-S.; Su, J.-H.; Yang, S.-J. *et al.* CN: 1,312,249, 2002.
- Gong, Y.-K.; Wei, Y.-F.; Dang, G.-C.; Lv, Y.-P. *Journal of Northwest University* **1997**, *27*, 49.
- Harris, J. T.; Hobbs, M. E. *J. Am. Chem. Soc.* **1954**, *76*, 1419.
- Zhang, X.-H.; Wang, L.-Y.; Zhai, G.-H.; Wen, Z.-Y.; Zhang, Z.-X. *J. Mol. Struct.* **2008**, *881*, 117.